Failures analysis of compressor blades of aeroengines due to service

Abstract

In spite of the high levels of reliability of modern aeroengine components resulting from rigid standards and practices, failures of compressor and turbine blades during normal operational environments are common situations which compromise the flight safety. The investigation of real failures affecting these components allows gaining a deeper knowledge concerning the mechanisms of crack initiation and propagation which, in turn, can be used in order to prevent future incidents or accidents.

This paper presents the analysis of two in service failures involving blades breakage belonging to different compressor stages. Crack growth mechanisms were evaluated based on the visual inspection of the affected components and with both macroscopic and microscopic observations of the fracture surfaces. The origins of crack initiation were evaluated through the examination of crack path and beach marks on the fracture surface.

Mechanical analyses were carried out to identify the possible causes of the failures by examining anomalies in the mechanical behaviour of the materials such as hardness tests, chemical composition and surface coating analysis through SEM observations.

The analysis of the different fracture surfaces shows that crack propagation is mainly related with fatigue mechanisms whilst crack initiation can be attributed to distinct causes, either the presence of defects in the surface of the blade due to

impact of debris or intrinsic material defects or some degrading mechanisms affecting the internal microstructure of the material. In some cases the blades were in service after having being object of an overhaul procedure, which can justify some crack initiation cases that caused in service failures.

1. Introduction

Aeroengine gas turbine components operate in a particularly aggressive environment where both high temperature and mechanical loading promote creep-fatigue damage at compressor blades. At the same time there is a continuous demand for higher thrust and lower fuel consumption and consequently each stage in the engine is required to work with higher loads without compromising safety. Therefore, the maximization of reliability levels of aeroengines is of paramount importance and several lifing procedures have been developed with this purpose [1]. However there is still a significant number of failures affecting critical components during normal operation and the rejection rate during overhaul for contention of incipient failure mechanisms is fairly high [2].

Compressor blades are within the most affected components for two main different reasons: either by the ingestion of debris, such as birds or sand, causing “Foreign Object Damages” (FOD) or by typical degrading mechanisms resulting from cyclic loading and high temperature environments (creep-fatigue

interaction). In the former case, the impact of small debris induces nicking of the blades which, in turn, will act as stress raisers prone to crack initiation [3]. Parallel to this, the damage caused by FOD tends to compromise the mechanical balance of the rotating components and also alters the aerodynamic flow over the blade airfoil leading to significant vibration or flutter which can promote crack propagation due to fatigue which, in turn, is a common cause of component breakage [2, 4].

The interaction of both creep and fatigue mechanisms is the other main cause of failure in compressors and turbines of aeroengines. Creep damage is a thermally activated and time dependent mechanism which results from structural changes leading to continuous reduction in the strength of the material during service mainly due to the formation of intergranular voids and subsequent cracking [5, 6]. By the other hand, fatigue crack propagation is a cyclic dependent mechanism occurring for temperatures below the creep range of the materials. In this case, a continuous plastic deformation process will extend to a size covering a significant region of the fracture surface with clear evidences of trangranular cracking and the formation of well defined striations. High temperature fatigue is an important issue when considering the mechanical behaviour of critical aeroengine components and there is a large bulk of investigations relating crack growth rates with different types of external effects, such as temperature, frequency of loading and cyclic stress ratio [7-10].

This paper presents the analysis of two cases where in service failures involving the breakage of blades belonging to different aeroengine compressor stages took place.

2 - Case A

In this case, some blades belonging to the fifth stage of a high pressure compressor have been fractured. The blade geometry and the blade failure location are shown in Fig. 1. The compressor blade breakage took place after 32625 hours (8897 cycles). The objective of this investigation is to undertake a failure analysis in order to determine and describe the factors responsible for the failures of these compressor blades, as well as to show that the proper application of failure analysis techniques can produce a valuable feedback to design and testing procedure improvements.

2.1 Material characterization

Different types of mechanical analyses were carried out in order to identify the possible causes of the failures by examining anomalies in the mechanical behaviour of the materials, such as chemical composition, hardness tests and surface coating analysis through SEM observations. One failed blade from the compressor stage shown in Figure 1 was provided for examination purposes.

2.1.1 Chemical composition

The chemical composition of the blade was determined using a scanning electronic microscopy (SEM) applying an X-ray spectrometry technique.

Table 1 gives the composition of the blade material considered in this study, which was referred by manufacturer of the engine as being Incoloy 901 nickel-base superalloy. The obtained material composition shows good agreement in comparison with the nominal values of Incoloy 901 [11].

2.1.2 Micro hardness

A micro-hardness evaluation of the material was performed using a *Shimadzu HMV-2* equipment with a Vikers type indenter and a load of 100g. A mean hardness value of 493HV was determined resulting from several measures at different places in the blade.

2.2 Examinations of fracture surface

Crack growth mechanisms were evaluated based on the visual inspection of the affected components and with both macroscopic and microscopic observations of the fracture surfaces.

2.2.1 Visual inspection

Fig. 2 shows a view of the fracture surface of the compressor blade mentioned in the previous sections. The fracture was developed in the normal plane of the blade axle and the tell-tale beach marks are indicative of clear fatigue mechanisms.

The crack propagated from the leading edge towards the trailing edge and from the lower surface towards the upper surface of the blade airfoil.

The beach marks reveal evidence of high cycle fatigue by blade vibration and dynamic stress as likely contributors to the failure. This indicates that there must have been a vibration condition sufficient to propagate cracking from initial defects formed at the leading edges of the blade.

2.2.2 Optical microscopy

The origins of crack initiation were evaluated through the examination of the crack path and beach marks present on the fracture surface.

The fracture surface is relatively plane and its area is about 2/3 of that of the total blade section (Fig. 3). As already explained, flat fracture surfaces are generally associated with fatigue damage where cycle dependent mechanisms prevail.

Therefore, the first step of this study was to locate the crack initiation site and on a second stage to look for the existence of crack propagation lines similar to those schematized in figure 4 [12]. These lines represent important points of load level variation or interruption during crack propagation until the final fracture of the component.

Fig. 5 and 6 show the fracture surface with six initial cracks on the lower surface of the blade, followed by a stable crack growth. The initial cracks propagated in different plans assuming a semi-elliptical shape.

The existence of multiple crack nucleation sites and the absence of any visible superficial nicks or other marks resulting from a possible foreign object impact suggest that fracture is mainly related with material defects.

The dimensions of crack propagation lines were measured using an X-Y table measuring facility coupled with a video monitor optical system allowing measurements with 0.01mm resolution (Table 2).

After the merge of the six initial cracks (crack depth-2 mm, crack length 23 mm) a fast crack propagation resulting from the increase of the stress intensity factor was observed.

2.2.3 Scanning electronon microscopy

Fig 7 presents the deformation lines observed by means of scanning electron microscopy (SEM). SEM observations confirmed that the initial defects at the leading edge were not formed by a corrosion pit. . As one can see, the fracture

surface of the blade shown in Fig. 8 has clear striation marks which are closely spaced and propagating on flat plateaus joined by shear steps (white arrow).

The image of the fracture surface of Fig. 9 was obtained with a higher magnification, allowing detecting fatigue striations indicative of the crack propagation direction, which in this case was found to be from the lower surface to the upper surface of the blade airfoil (black arrow).

Figure 10 is another image of the fracture surface where a typical transgranular crack path with ductile fatigue striations is clearly visible. Fig. 11 reports to this same region but higher magnification allows detecting secondary cracking.

Finally, some evidences of brittle fracture near the final fracture region is observed in Fig. 12, as well as pronounced radial marks indicating the direction of crack propagation.

3 - Case B

This study refers to the failure analysis of a turbine engine occurred in service. The analysis after the observation of the engine interior, implied that most of the blades downward the 5^{th} stage were severely damaged. The observation of the fracture blades allowed concluding that all the blades except one had failed by sudden fracture. One of the blades in the 5^{th} stage of the compressor of the aero engine had a substantially different fracture surface where characteristics of a fatigue failure were easily observed. Therefore the first conclusion was that a blade on the 5^{th} stage had failed by fatigue and induced the failure of subsequent

blades of the compressor. The main analysis of this study is related with the observations and comments that were carried out on the blade that fractured due to fatigue. The material was identified as a martensitic stainless steel 17-4PH.

Figure 13 shows the fracture surface of the blade that failed by fatigue.

The fracture developed in a plane normal to the blade axis and it can be observed that the major part of the surface is smooth with several beach marks present on the fracture surface, having a semi-elliptic shape starting from the convex part of the blade. These marks are related with different crack growth phases starting from one or more points corresponding to crack initiation. Only a very small part of the surface is occupied by fast fracture, meaning that the failure was due to fatigue with low stress levels.

Two radial marks are also observed on the fracture surface. These marks correspond to the intersection of different fatigue crack propagation planes that formed one single fracture surface by joining together after a previous slow crack growth phase. Three cracks can be easily identified on the fractured surface merging on the radial direction and forming a final crack which, in turn, led to a faster crack growth rate with a subsequent final failure. This area is shown with major amplification on figure 14.

For two of these cracks it was possible to identify the initiation site. An example of the local of crack initiation for crack nº1 of figure 13 is shown on figures 15 and 16, corresponding to a pitting area on the surface of the blade.

It is interesting to refer that it was not possible to identify any beach marks of crack propagation for small dimensions of the crack, typically with a length of 1.8 mm and depth of 0.9 mm in the case of crack nº 1. This fact corresponds to a very slow crack growth and therefore it is not possible to observe different crack growth stages. When the three cracks merge to form the final crack it can be easily observed some beach marks corresponding to different stages of crack propagation during a fast crack growth process. A minimum of 13 and a maximum of 15 beach marks were identified on the surfaces of fracture for this crack propagation phase.

4. Conclusions

Case A:

- Both chemical composition analysis and micro hardness evaluation confirmed that the material of the blade is a nickel-base superalloy (Incoloy 901);

- The crack propagated from the leading edge towards the trailing edge and from the lower surface towards the upper surface of the blade. During propagation, some striation marks were visible revealing evidence of high cycle fatigue induced by blade vibration and dynamic stress as likely contributors to the failure. This indicates that there must have been a vibration condition sufficient to promote crack propagation from initial defects formed at the leading edge of the blade;

- The multiple crack nucleation and the nonexistence of a foreign object impact point suggest that fracture is related to material defects.

Case B:

- This analysis refers to a failure of a blade in the 5^{th} stage of an aeroengine that fractured by fatigue. Three fatigue cracks were identified and crack initiation was determined for each of the three cracks; the initiation sites were identified as pits on the blade convex surface, probably due to impact of debris.
- Propagation of the different cracks occurred by slow crack growth and no beach marks were identified but when the cracks joined in a single one, faster crack growth has occurred and beach marks are visible on the fractured surface.
- The major area of the failure surface was identified as fatigue crack growth and only a residual one was identified as fast fracture, therefore a low stress level intensity on the blade may be considered.

5. References

[1] Harrison, G.F., Tranter, P.H.; “Stressing and Lifing Techniques for High Temperature Aeroengine Components”; Mechanical Behaviour of Materials at High Temperature (edited by C, Moura Branco et al.); NATO ASI Series; Kluwer Academic Pub.; Netherlands; 1996.

[2] Carter, T.; “Common Failures in Gas Turbine Engines”; Engineering Failure Analysis, 12; Elsevier; 2005; pp 237-247.

[3] Chen, X.; “Foreign Object Damage on the Leading Edge of a Thin Blade”; Mechanics of Materials, 37; Elsevier; 2005; pp 447-457.

[4] Liu, X.L., Zhang, W.F., Jiang, T., Tao, C.H.; “Fracture Analysis on the 4th Compressor Disc of Some Engine”; Engineering Failure Analysis, 14; Elsevier; 2007; pp 1427-1434.

[5] Sklenicka, V.; “Development of Intergranular Damage Under High Temperature Loading Conditions”; Mechanical Behaviour of Materials at High Temperature (edited by C. Moura Branco et al.); NATO ASI Series; Kluwer Academic Pub.; Netherlands; 1996; pp 43-58.

[6] Webster, G.A., Ainsworth, R.A.;”High Temperature Component Life Assessment”; Chapman & Hall; U.K.; 1994.

[7] Winstone, M.R., Nikbin, L.M., Webster, G.A.; “Modes of Failure under Creep/Fatigue Loading of a Nickel-Based Superalloy”; Journal of Materials Science, Vol. 20; 1985; pp 2471-2476.

[8] Evans, W.J., Jones, J.P., Williams, S.; “The Interactions Between Fatigue, Creep and Environment Damage in Ti 6246 and Udimet 720Li”; International Journal of Fatigue, Vol. 27; Elsevier; 2005; 1473-1484.

[9] Onofrio, G., Osinkolu, G.A., Marchionni, M.; “Effects of Loading Waveform on Fatigue Crack Growth of Udimet 720Li Superalloy”; International Journal of Fatigue, Vol. 26; Elsevier; 2004; 203-209.

[10] Pang, H.T., Reed, P.A.S.; “Fatigue Crack Initiation and Short Crack Growth in Nickel-base Turbine Disk Alloys – The Effect of Microstructure and Operating

Parameters”; International Journal of Fatigue, Vol. 25; Elsevier; 2003; 1089-1099.

[11] Fecht, H., Furrer, D., “Processing of Nickel-Base Superalloys for Turbine Engine Disc Applications”, Advanced Engineering Materials, Vol. 2, Nº 12, 2000, pp. 777-787.

[12] “Failure Analysis Library”, ASM international, The Materials Information Society, 1996.

Figure 1 – Blade geometry and location of failures.

Figure 2 – Fracture surface of the blade.

Figure 3 – Morphology of fracture surface of the blade.

Figure 4 – Scheme of typical crack propagation lines [12].

Figure 5 – Crack propagation lines observed in the fracture surface of the blade.

Figure 6 – Final fracture region observed in the fracture surface of the blade.

Figure 7 – Fracture surface of the blade observed by scanning electronic microscopy.

Figure 8 – High-cycle fatigue striations in the fracture surface of the blade. The striation are closely spaced and propagate on flat plateaus joined by shear steps (white arrows); black arrow indicates direction of crack propagation.

Figure 9 – Fatigue striations with higher magnification as obtained in the fracture surface of the blade. The black arrow indicates the direction of crack propagation.

Figure 10 – The fracture path is transgranular with ductile fatigue striations. The crack propagation direction is indicated by the black arrow.

Figure 11 – Same region of interest presented in Fig.10 (but now with higher magnification) showing secondary cracks.

Figure 12 – Brittle fracture observed near the final fracture zone. The pronounced radial marks indicate the fracture directions.

Figure 13 - Crack propagation lines observed in the fracture surface of the blade.

Figure 14 – Identification of the radial marks on the fracture surface.

Figure 15 – Identification of crack initiation and beach marks.

Figure 16 – View of crack initiation site on the blade surface.

Table 1 – Chemical composition of the compressor blade and nominal values of superalloy Incoloy 901 [11].

Table 2 – Dimensions of crack propagation lines observed in the fracture surface of the blade.

Figure 1

Figure 2

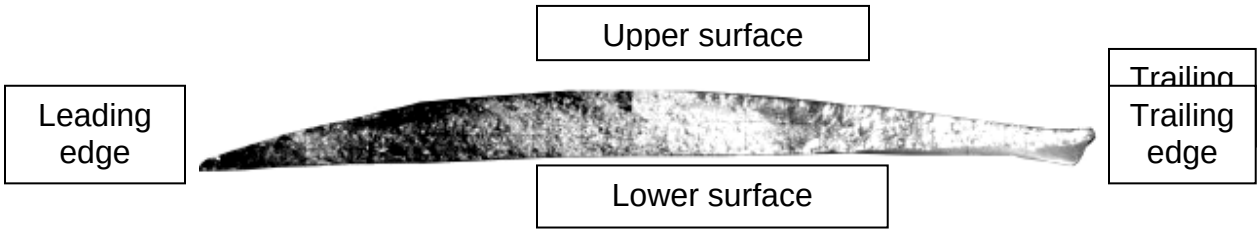

Figure 3

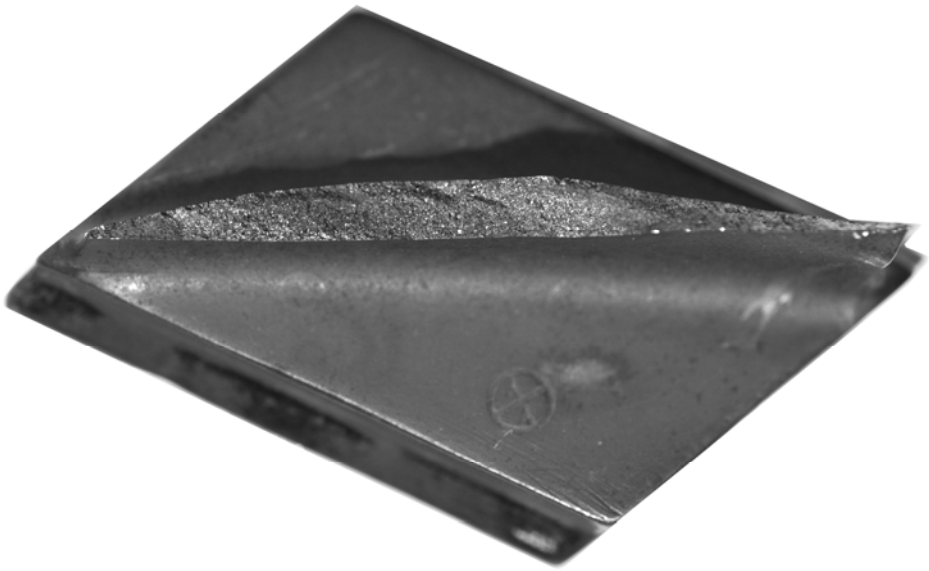

Figure 4

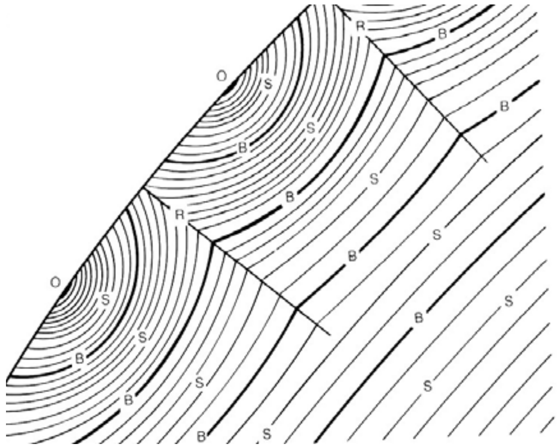

Figure 5

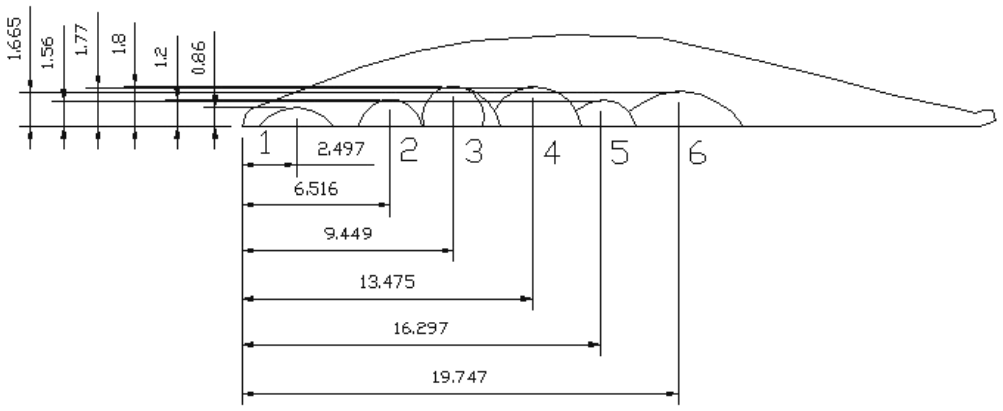
1.665
1.56
1.77
1.8
1.2
0.86
1
2.497
2
3
4
5
6
6.516
9.449
13.475
16.297
19.747

Figure 6

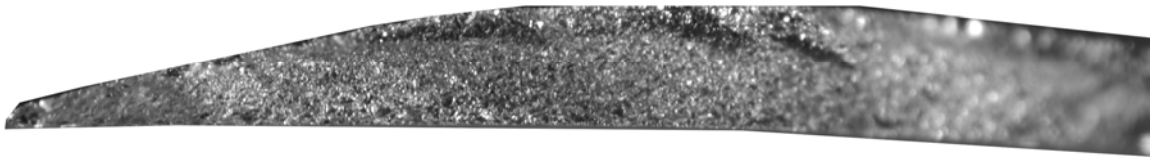

Figure 7

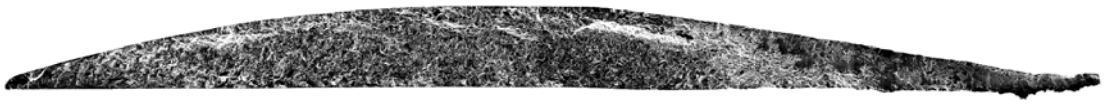

Figure 8

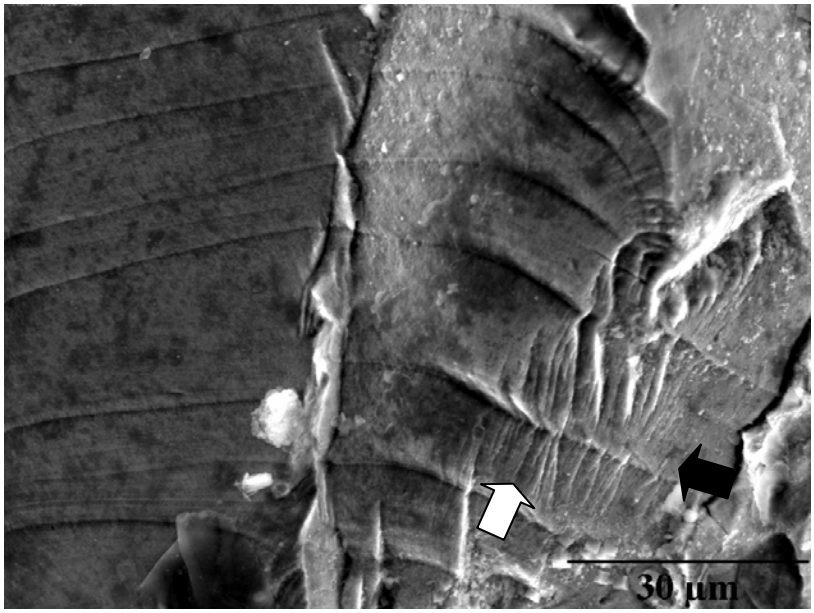

Figure 9

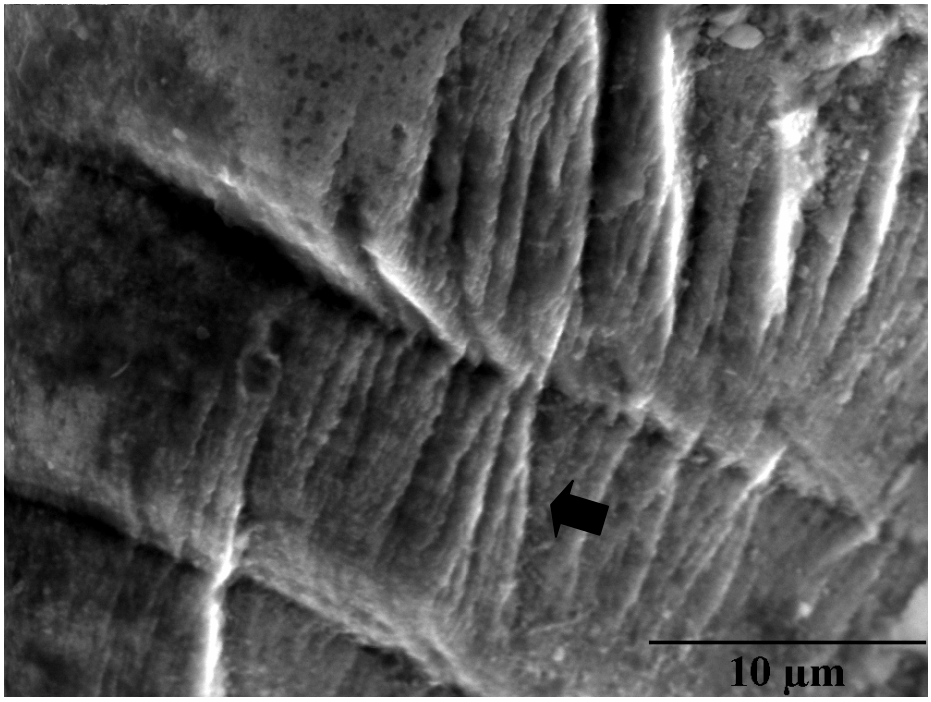

Figure 10

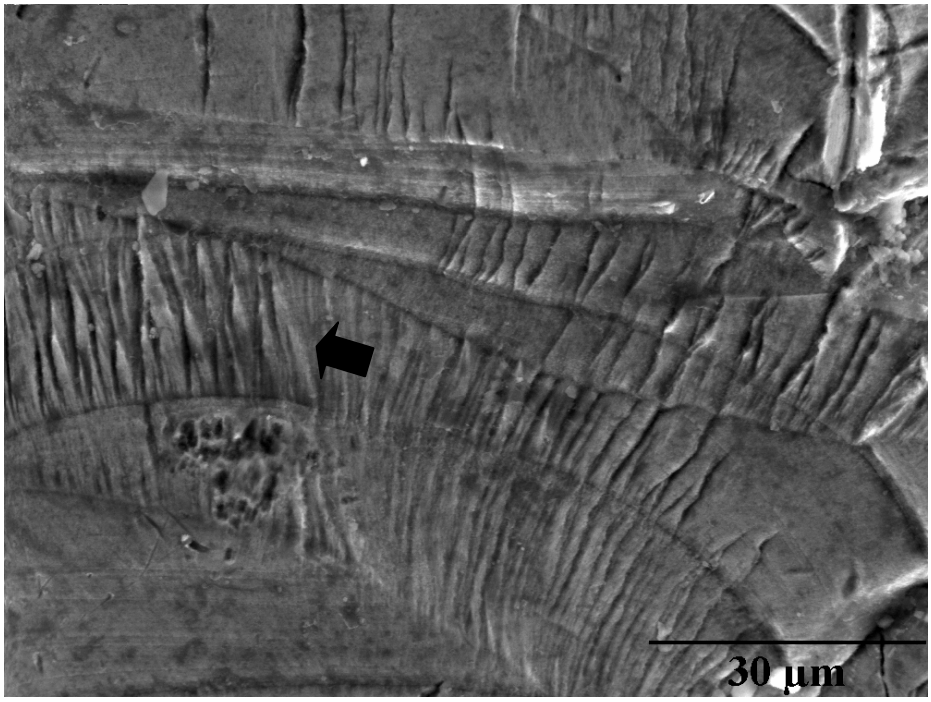

Figure 11

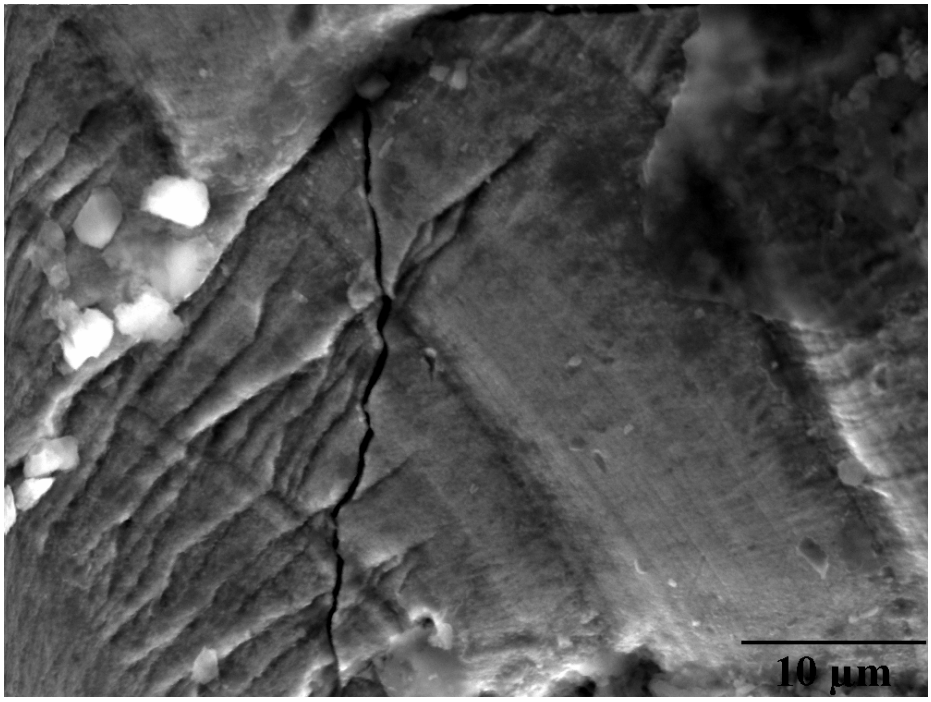

Figure 12

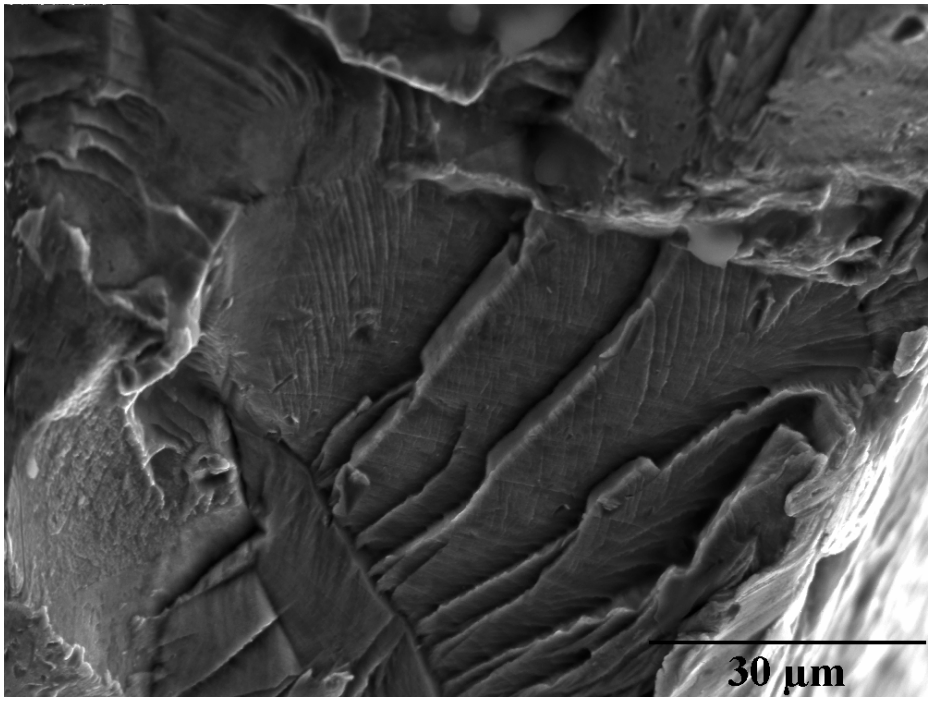

Figure 13

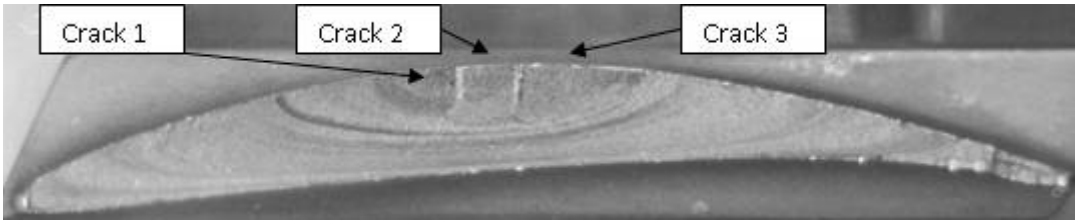

Figure 14

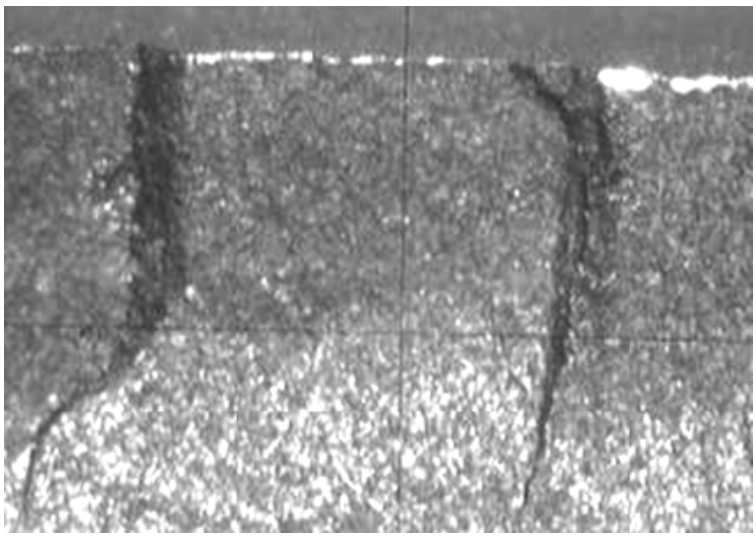

Figure 15

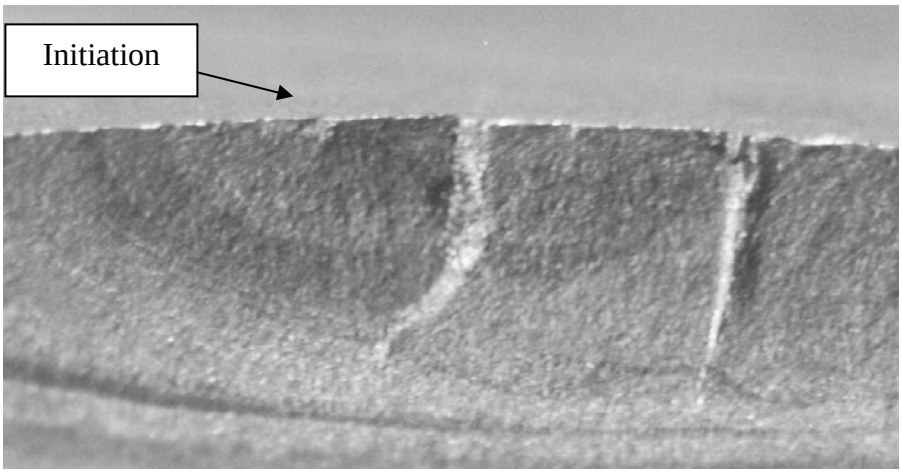

Figure 16

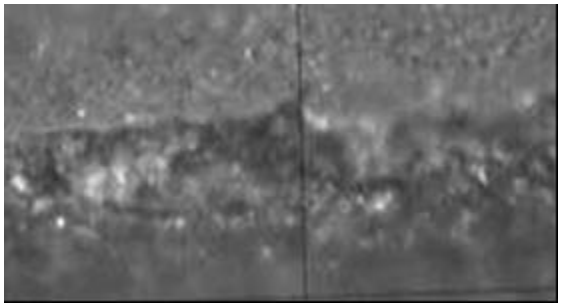

Table 1

Chemical element [%]	Fe	Ni	Cr	Ti	Mo
Analyzed	43.18	46.14	13.67	3.04	5.52
Nominal	36.2	42.5	12.5	2.7	6

Table 2

Crack	Surface crack length [mm]	Crack depth [mm]	Distance from nucleation point to leading edge [mm]
1	3.40	0.86	2.50
2	2.94	1.20	6.52
3	2.67	1.80	9.45
4	3.54	1.77	13.47
5	2.84	1.56	16.30
6	5.56	1.66	19.75